Aalborg Universitet

AALBORG UNIVERSITY
DENMARK

Blind Multi-Band Spectrum Signals Reconstruction Algorithms Comparison

Shen, Hao; Arildsen, Thomas; Larsen, Torben

BLIND MULTIBAND SPECTRUM SIGNALS RECONSTRUCTION ALGORITHMS COMPARISON

Hao Shen[1], Thomas Arildsen[1], Deepaknath Tandur[2], and Torben Larsen[1]

[1]Aalborg University
Dept. of Electronic Systems
DK-9220 Aalborg, Denmark
E-mail: {hsh; tha; tl}@es.aau.dk

[2]Agilent Technologies, Belgium
E-mail: deepaknath_tandur@agilent.com

ABSTRACT

This paper investigates sparse sampling techniques applied to downsampling and interference detection for multiband radio frequency (RF) signals. To reconstruct a signal from sparse samples is a compressive sensing problem. This paper compares three different reconstruction algorithms: 1) ℓ_1 minimization; 2) greedy pursuit; and 3) MUltiple SIgnal Classification (MUSIC). We compare the performance of these algorithms and investigate the robustness to noise effects. Characteristics and limitations of each algorithm are discussed.

1. INTRODUCTION

According to traditional Shannon-Nyquist sampling theory, to allow perfect reconstruction, a signal must be sampled at more than twice the highest frequency contained in the signal, also known as the Nyquist rate [1].

In traditional spectrum analyzers, a narrow band signal is usually converted to baseband and then sampled according to the Nyquist rate. However, when the signal is affected by interference or frequency shifting effects, down-converting the signal to baseband may introduce aliasing unless an anti-aliasing filter is applied. On the other hand, to sample such RF signals at Nyquist rate (e.g. 100 GHz) is usually very difficult or impossible in practice. Therefore, reducing the sampling rate is highly needed.

In order to reduce the sampling rate, the signal structure should be studied first. Suppose a bandpass signal occupies a spectrum from $f_{a,1}$ to $f_{b,1}$. Meanwhile, several interference signals are randomly allocated in the intervals $[f_{a_i}, f_{b_i}]$, $i = 2, \ldots, N$, where $f_{a,1} < \cdots < f_{a,N}, f_{b,1} < \cdots < f_{b,N}$. Then, the Nyquist sampling rate for such signal is $f_{nyq} = 2f_{b,N}$. According to the theory of compressive sensing [2], a signal can be reconstructed from far fewer samples, i.e. below the Nyquist rate, if the signal is sparse in a certain domain. Since it is known that there are only N frequency bands in the entire spectrum, and the width of each band is $B_1 = f_{b,1} - f_{a,1} > 0, \ldots, B_N = f_{b,N} - f_{a,N} > 0$, the signal spectrum can be regarded as sparse if $\sum_{i=1}^{N} B_i \ll f_{nyq}$. Therefore, compressive sensing can theoretically be applied to reconstruct a multiband RF signal using a sampling rate significantly below the Nyquist rate.

In practice, the number of subbands N and the location of the subbands are unknown for interference signals. It be-

comes a blind multiband signal reconstruction (BMSR) problem, which was first discussed by Feng in 1996 [3]. In 2009, Mishali and Eldar applied compressed sensing theory to the BMSR problem [4]. They formulated the problem as a multiple measurement vector (MMV) problem. Chen and Huo later applied convex optimization and greedy pursuit to solve the MMV problem [5].

In this paper, we mainly investigate three reconstruction algorithms to solve the BMSR problem. The first is a general MUSIC algorithm, which is very suitable for the BMSR problem [6]. The other two are widely used reconstruction algorithms in traditional compressive sensing theory. One is Multiple Basis Pursuit De-Noising (M-BPDN) [7], which belongs to the family of ℓ_1-minimization in convex optimization, and the other belongs to the category of greedy pursuit algorithms. Instead of using multi-orthogonal matching pursuit (M-OMP) [5], we apply a stagewise factor as Multiple Stagewise Orthogonal Matching Pursuit (M-StOMP) [8]. Then, we investigate the performance of these algorithms from the view of detecting spectrum allocation and evaluate the mean square error (MSE) in the frequency domain between the reconstructed signal and the signal sampled at Nyquist rate. We also investigate the robustness of these algorithms under various levels of additive white Gaussian noise (AWGN). Finally, the disadvantages and limitations of each algorithm are listed.

2. PROBLEM AND BACKGROUND

2.1 Single Measurement Vector Model

In compressive sensing [2], one single measurement vector model is given by,

$$\mathbf{y} = \mathbf{A}\mathbf{x}, \tag{1}$$

where $\mathbf{y} \in \mathbb{C}^{p \times 1}$, $\mathbf{A} \in \mathbb{C}^{p \times L}$, $\mathbf{x} \in \mathbb{C}^{L \times 1}$, and $p < L$. Suppose $\zeta \in \mathbb{C}^{L \times 1}$ is a linear transformation of the signal x in the basis $\mathbf{\Psi}$, $\zeta = \mathbf{\Psi}\mathbf{x}$, and $\mathbf{x} = \mathbf{\Psi}^{-1}\zeta$. If $\|\mathbf{x}\|_0 = q$, and $q \ll L$, $\mathbf{x}$ is a sparse representation of ζ, and $\mathbf{\Psi} \in \mathbb{C}^{L \times L}$ is the dictionary matrix of ζ. Here $\| \cdot \|_0$ is a zero norm calculation, which is defined as, $\|\mathbf{x}\|_0 = T, T = \{i | x_i \neq 0\}$. Transforming the signal ζ by the measurement matrix $\mathbf{\Phi} \in \mathbb{R}^{p \times L}$, the compressed vector $\mathbf{y}$ is obtained: $\mathbf{y} = \mathbf{\Phi}\zeta$. Then, the matrix $\mathbf{A}$ in (1) is $\mathbf{A} = \mathbf{\Phi}\mathbf{\Psi}$.

2.2 Multiple Measurement Vector Model

The MMV problem is an extension of the single measurement vector problem as follows [5]:

$$\mathbf{Y} = \mathbf{A}\mathbf{X}, \tag{2}$$

where $\mathbf{Y} \in \mathbb{C}^{p \times B}$, $\mathbf{A} \in \mathbb{C}^{p \times L}$, $\mathbf{X} \in \mathbb{C}^{L \times B}$.

Here $\mathbf{A}$ is a similar combination matrix as in (1), with $p < L$. $\mathbf{X}$ is a row-sparse matrix, i.e., has few non-zero rows, and $\mathbf{Y}$ is an observed matrix. The vectors $\hat{\mathbf{x}}_i$ and $\hat{\mathbf{y}}_i$, $i = 1, \ldots, B$, are the columns of $\mathbf{X}$ and $\mathbf{Y}$. When $B = 1$, (2) reduces to the single measurement vector problem. Therefore, the MMV problem can be regarded as solving B parallel single measurement vector problems. (2) can be rewritten as,

$$\hat{\mathbf{y}}_i = \mathbf{A}\hat{\mathbf{x}}_i, \quad i = 1, \ldots, B. \tag{3}$$

Meanwhile, considering the effect of AWGN ϵ, (2) is extended by,

$$\mathbf{Y} = \mathbf{A}\mathbf{X} + \epsilon, \tag{4}$$

where $\epsilon \sim \mathcal{N}(0, \frac{1}{B}\delta_\varepsilon^2)$, and $\mathbb{E}[\varepsilon_i \varepsilon_i] = \delta_\varepsilon^2$.

2.3 Multiband Signal Model

Here, we use a multiband signal model [9]. Suppose $x(f)$ is the spectrum of $\zeta(t)$. Let $\mathcal{F}$ denote the spectrum support set in the whole spectrum $[0, f_{nyq}]$. We define a signal as multiband if $\mathcal{F} = \bigcup_{i=1}^{N}[f_{a,i}, f_{b,i}]$, and $x(f_n) = 0$, if $f_n \notin \mathcal{F}$. Since the maximum frequency $f_{b,N}$ in $\mathcal{F}$ is unknown, the signal is bandlimited to f_{nyq}. As mentioned before, the spectrum of a signal is sparse if $\sum_{i=1}^{N} B_i \ll f_{nyq}$. How to sample this kind of signal in a sparse way is discussed below.

Instead of using one sampler on $\zeta(t)$ uniformly at the Nyquist rate, i.e. $\zeta[n] = \zeta(nT)$, $T = 1/f_{nyq}$, Feng and Bresler proposed a parallel structure with p samplers [3]. Each one samples at rate of $1/(LT)$ with a different time shifting. Consequently, the $x(f)$ in frequency is divided into L consecutive subbands, i.e. $x_i(f_i)$, $f_i \in [\frac{i-1}{LT}, \frac{i}{LT})$, $i = 1, \ldots, L$.

Then, the $x(f)$ is reformulated as $X(\hat{f}), \hat{f} \in [0, \frac{1}{LT})$ (details in [4]). Each row of $X(\hat{f})$ is $x_i(\hat{f})$, $i = 1, \ldots, L$, which corresponds to $x_i(f_i)$. Suppose the bandwidth of each subband in $x(f)$ does not exceed a maximum bandwidth B_{max}, the maximum $\hat{f}$ should be larger than B_{max}, i.e. $\max\{B_i\} \leq B_{max} \leq 1/(LT)$. Here we discretize the $\hat{f}$ to B samples with $B \geq B_{max}$, we get $\mathbf{X} \in \mathbb{C}^{L \times B}$, and $L \leq 1/(BT)$. Then, the model of multiband signal is given by,

$$\mathbf{Y} = \mathbf{A}\mathbf{X}, \tag{5}$$

where $\mathbf{A} \in \mathbb{C}^{p \times L}$ is referred as a universal sampling matrix [3]. The structure can be a multicoset sampler [3] or a random demodulator [10]. Here p is the number of samplers, and L is the sampling period. The overall sampling rate is $f_s = \frac{p}{LT} = \frac{p}{L}f_{nyq}$, with $p < L$. It is clear that (5) is exactly the same type of problem (MMV) as (2).

In this paper, the investigated reconstruction algorithms are based on the discretized frequency model (2). As long as $\mathbf{X}$ is reconstructed, ζ can be easily calculated [4]. The effects of frequency discretization and quantization are out of the scope of this paper, as well as the design of the $\mathbf{A}$ matrix.

2.4 Optimization Problem

Since $p < L$, (2) is an underdetermined equation, satisfied by infinitely many solutions. Therefore a unique solution of (3) should be the sparsest $\hat{\mathbf{X}}$.

To reconstruct the original signal from the observed signal, several algorithms have been proposed in the literature. The sparsest solution to (2) can be found by solving the below optimization problem,

$$\begin{aligned} \min \quad & \|\mathcal{R}(\mathbf{X})\|_0 \\ \text{subject to} \quad & \mathbf{Y} = \mathbf{A}\mathbf{X}, \end{aligned} \tag{6}$$

where $\mathcal{R}(\cdot)$ calculates the ℓ_2 norm of the ith row in $\mathbf{X}$, $i = 1, \ldots, L$, and $\|\mathcal{R}(\cdot)\|_0$ returns the number of rows containing non-zeros elements.

Here recall the multiband signal model. Before reformulating the frequency, the sparsity $q = \|\mathbf{x}\|_0$ in (1) counts the number of non-zero frequencies in the whole spectrum. However, in (5), $N = \|\mathcal{R}(\mathbf{X})\|_0, N = 1, \ldots, L$, is the number of subbands allocated in the support $\mathcal{F}$.

3. RECONSTRUCTION ALGORITHMS

We define S as the support of $\mathbf{X}$, $S \triangleq \{i| \|\mathbf{x}_i\|_0 \neq 0\}$, where $\mathbf{x}_i$ is the ith row of $\mathbf{X}$. In the MMV problem, we have $\mathbf{X}^S \triangleq [\hat{\mathbf{x}}_1^H, \ldots, \hat{\mathbf{x}}_N^H]^H$, where $\hat{\mathbf{x}}_i = \mathbf{x}_{S[i]}, i = 1, \ldots, N$. $\mathbf{x}_j$ is the jth row of $\mathbf{X}$, and $(\cdot)^H$ is the Hermitian transpose. Correspondingly, $\mathbf{A} = [\mathbf{a}_1, \cdots, \mathbf{a}_L]$, where $\mathbf{a}_i$ is the ith column in $\mathbf{A}$. Then, $\mathbf{A}_S \triangleq [\hat{\mathbf{a}}_1^H, \cdots, \hat{\mathbf{a}}_N^H]$, where $\hat{\mathbf{a}}_i = \mathbf{a}_{S[i]}$.

Obviously, if the support S is known, (2) reduces to,

$$\mathbf{Y} = \mathbf{A}_S\mathbf{X}^S, \tag{7}$$

where $\mathbf{A}_S \in \mathbb{C}^{p \times N}$, and $\mathbf{X}^S \in \mathbb{C}^{N \times B}$. If $p > N$, (7) becomes an overdetermined equation. Then, $\hat{\mathbf{X}}$ can be reconstructed as the least-squares estimate

$$\hat{\mathbf{X}} = \mathbf{A}_S^\dagger\mathbf{Y}, \tag{8}$$

where $(\cdot)^\dagger$ is the pseudoinverse operation.

However, S is usually unknown in (2). To solve (6) is an NP-hard combinatorial optimization problem [5], since $\binom{L}{N}$ combinations must be evaluated to find the correct support S. This computation increases exponentially with the size L, and N. For multiband signal models, when S is unknown, (5) becomes a blind spectrum signal model. Therefore, many suboptimal algorithms are proposed to reconstruct S and X.

The other problem is how to be sure that $\hat{\mathbf{X}}$ is the sparsest solution of (6) even if support S is reconstructed. Will there exist another solution $\tilde{\mathbf{X}}$ such that $\|\tilde{\mathbf{X}}\|_0 < \|\hat{\mathbf{X}}\|_0$? Therefore, some properties of the matrix $\mathbf{A}$ should be discussed to meet the uniqueness condition of (5).

3.1 Uniqueness and Minimum Sampling Rate

By following the theorem and definition of Kruskal-rank of the matrix $\mathbf{A}$ in [4], we have:

Definition 1 Kruskal-rank: *Given a matrix $\mathbf{A}$, define $\eta = \text{KruskR}(\mathbf{A})$ as the maximal number such that every η columns of matrix $\mathbf{A}$ are linearly independent.*

Theorem 1 Uniqueness: *The matrix $\mathbf{X}$ is the unique sparsest solution of (6), if $\|\mathcal{R}(\mathbf{X})\|_0 \leq \text{KruskR}(\mathbf{A})/2$.*

Calculating the Kruskal-rank of a matrix $\mathbf{A}$ is a combinatorial problem. In this paper, we apply a universal sampling matrix $\mathbf{A}$ which guarantees that $\mathbf{X}$ is uniquely reconstructable [3]. For a specific number of samplers p, one distinct sampling matrix $\mathbf{A}$ is found via solving a minimax optimization problem. For details, please refer to [3].

Regarding to the minimum sampling rate, since $\mathbf{A} \in \mathbb{C}^{p \times L}$ with $p < L$, it is easy to get $p \geq \eta \geq 2\|\mathcal{R}(\mathbf{X})\|_0 = 2N$.

Theorem 2 Minimum rate: *The theoretical minimum sampling rate of the overall parallel structure is* $f_s = 2\frac{\|\mathcal{R}(\mathbf{X})\|_0}{L} f_{nyq}$.

In the following parts, we discuss how to reconstruct the support S, and solve (4) by three suboptimal algorithms.

3.2 MUSIC with Spectral Analysis

MUSIC is a technique of spectral estimation, which was first invented by Schmidt [6] in 1986 to solve the problem of direction-of-arrival (DOA). In this paper, we use the traditional MUSIC algorithm [4] to solve (2). The detailed steps are listed in Algorithm 1.

Algorithm 1 MUSIC Algorithm

Input: $\mathbf{A}, \mathbf{Y}$, and N
1: Estimate the autocorrelation, $\mathbf{Q} = \mathbb{E}\left[\mathbf{Y}\mathbf{Y}^H\right]$
2: Eigendecomposition, $\mathbf{Q} = \mathbf{U}\mathbf{\Lambda}\mathbf{U}^H$
3: Find the $2N$ signal subspace, $\mathbf{U}_s = \mathrm{sub}_{\mathrm{sig}}(\mathbf{U})$
4: Calculate the MUSIC spectrum,
   $\hat{P}_{mu} = \left\{\mathbf{a}_i^H(\mathbf{I} - \mathbf{U}_s\mathbf{U}_s^H)\mathbf{a}_i\right\}^{-1}$, $i = 1, ..., L$
5: Set S as the indices of peak values of $\hat{P}_{mu}$
6: **return** S and $\hat{\mathbf{X}} = \mathbf{A}_S^\dagger \mathbf{Y}$

In step 2, $\mathbf{Q}$ is decomposed as, $\mathbf{Q} = \mathbf{U}\mathbf{\Lambda}\mathbf{U}^H$, or $\mathbf{Q} = \sum_{i=1}^{p} \lambda_i \mathbf{u}_i \mathbf{u}_i^H$. One of the crucial steps in MUSIC is to separate the signal subspace and noise subspace from $\mathbf{U}$. For the noiseless case, the order of eigenvalues is,

$$\lambda_1 \geq \lambda_2 \geq \cdots \geq \lambda_{2N} \geq \lambda_{2N+1} = \cdots = \lambda_p = 0, \quad (9)$$

Then, in step 3, the first $2N$ eigenvalues, $\lambda_i, i = 1, \ldots, 2N$, are referred as signal subspace eigenvalues, and $\mathbf{u}_i, i = 1, \ldots, 2N$, are referred as signal subspace eigenvectors.

However, with increasing noise level ϵ, the difference between signal eigenvalues and noise eigenvalues is more and more difficult to distinguish, which affects the performance of MUSIC dramatically.

3.3 Basis Pursuit Minimization

Basis pursuit [11] is a convex relaxation of ℓ_0 minimization in (6),

$$\begin{aligned} \min \quad & \|\mathcal{R}(\mathbf{X})\|_1 \\ \text{subject to} \quad & \mathbf{Y} = \mathbf{A}\mathbf{X}. \end{aligned} \quad (10)$$

Considering the effect of noise (4), basis pursuit de-noising (BPDN) is an approximation of basis pursuit,

$$\begin{aligned} \min \quad & \|\mathcal{R}(\mathbf{X})\|_1 \\ \text{subject to} \quad & \|\mathbf{y}_i - \mathbf{A}\mathbf{x}_i\|_2^2 \leq \delta_\epsilon^2, i = 1, \cdots, B. \end{aligned} \quad (11)$$

In this paper, we use the function `spgl1_mmv` from the SPGL1 toolbox to solve the BPDN in MMV problem [7].

3.4 Greedy Pursuit

Orthogonal matching pursuit (OMP) is an improvement of matching pursuit (MP) [12]. In relation to the MMV problem, several greedy algorithms have been proposed [5]. One of the improved M-OMP is listed in Algorithm 2 [5].

Algorithm 2 Multi-orthogonal matching pursuit (M-OMP)

Input: residual $R^{(0)} = \mathbf{Y}$, subset $S^0 = \emptyset$, iteration $n = 1$
1: **while** stop criterion is not met **do**
2:   $\mathbf{g}_i^{(n)} = \mathbf{R}^{(n-1)^H}\mathbf{a}_i$
3:   $S^{(n)} = S^{(n-1)} \cup \arg_i \max \left\|\mathbf{g}_i^{(n)}\right\|_r$
4:   $\mathbf{X}_{S^{(n)}}^{(n)} = \mathbf{A}_{S^{(n)}}^\dagger Y$
5:   $\mathbf{R}^{(n)} = \mathbf{Y} - \mathbf{A}\mathbf{X}^{(n)}$
6:   check stop criteria
7:   $n := n + 1$
8: **end while**
9: **return** $\mathbf{X}$ and S

In Algorithm 2, $S^{(n)}$ denotes a set containing the indices of the elements selected up to n^{th} iteration. $\mathbf{R}^{(n)}$ is the residual in the nth iteration. $\mathbf{g}_i$ is the projection of the residual on the ith column of $\mathbf{A}$. The main change of the M-OMP in [5] is the step 3, where $\|\cdot\|_r$ calculates the r-norm of $\mathbf{g}_i$. In this paper, we set $r = 2$.

Usually, when $\mathbf{A}$ is not an orthogonal basis, the orthogonality of M-OMP is not preserved. In step 3, it is unnecessary to find a new column vector of $\mathbf{a}_i$, which must be orthogonal to the previous ones. By introducing the concept of a stagewise weak factor λ [8], we change step 3 in Algorithm 2, resulting in Algorithm 3. Instead of selecting the index with max $\|\mathbf{g}_i\|_r$, we select indices which are no less than $\lambda \cdot \|\mathbf{g}_i\|_r$, where $\lambda = 0, \ldots, 1$. When $\lambda = 1$, Algorithm 3 is exactly the same as Algorithm 2.

Algorithm 3 Multiple Stagewise Orthogonal Matching Pursuit (M-StOMP)

Input: residual $\mathbf{R}^{(0)} = Y$, subset $S^0 = \emptyset$, λ, iteration $n = 1$
1: **while** stop criterion is not met **do**
2:   $\mathbf{g}_i^{(n)} = \mathbf{R}^{(n-1)^T}\mathbf{a}_i$
3:   $S^{(n)} = S^{(n-1)} \cup \left\{i : \left\|\mathbf{g}_i^{(n)}\right\|_r \geq \lambda \max_i \left\|\mathbf{g}_i^{(n)}\right\|_r\right\}$
4:   $\mathbf{X}_{S^{(n)}}^{(n)} = \mathbf{A}_{S^{(n)}}^\dagger \mathbf{Y}$
5:   $\mathbf{R}^{(n)} = \mathbf{Y} - \mathbf{A}\mathbf{X}^{(n)}$
6:   check stop criteria
7:   $n := n + 1$
8: **end while**
9: **return** $\mathbf{X}$ and S

---

4. NUMERICAL EXPERIMENTS

In this section, we discuss the performance of each algorithm. First, we describe the simulation set-up. Second, two aspects of performance are discussed.

4.1 Simulation Set-up

Fig. 1 shows the spectrum of a multi-band signal. We set the entire bandwidth as 5 kHz. The Nyquist frequency is $f_{nyq} = 1/T = 10$ kHz. There are $N = 3$ subbands in total. We set the maximum bandwidth of each bandwidth $B_i \leq 200$ Hz. Since the number of allocated subbands 3, 6 samplers are used, and each sampling at the rate $1/(LT)$, where $L \leq 1/(BT) = 50$, so $1/(LT) = 200$ Hz. The overall sampling rate is $p/LT =$
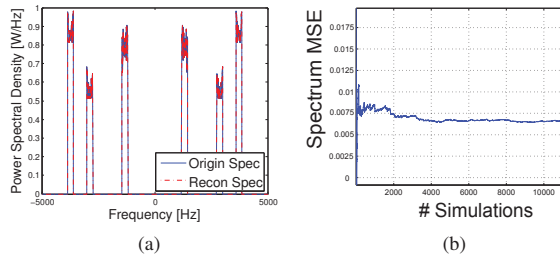
Figure 1: Simulated signal containing 3 subbands with each bandwidths $\leq 200\,\mathrm{Hz}$. Entire bandwidth $5\,\mathrm{kHz}$. 6 samplers. Overall sampling rate $1.2\,\mathrm{kHz}$. (a) Original vs. reconstructed spectrum by MUSIC. (b) MUSIC algorithm benchmark at $\mathrm{SNR_{in}} = 100\,\mathrm{dB}$.

$6 \cdot 200\,\mathrm{Hz} = 1200\,\mathrm{Hz}$, which is the minimum sampling rate f_s in theorem 2. Apart from the number of samplers and input signal to noise ratio (SNR), the other parameters are fixed in the simulation set-up.

In Fig. 1a, the blue line is the original spectrum with $100\,\mathrm{dB}$ as input SNR. The red dashed line is the spectrum reconstructed by the MUSIC algorithm. We can see that the spectrum support is perfectly reconstructed at the minimum sampling rate when $p = 6$. The noise applied is AWGN. By changing the input SNR ($\mathrm{SNR_{in}}$) level, we can check the robustness of the reconstruction algorithms. However, since the allocation of the signal subbands is unknown, the noise is added on the entire signal spectrum. Therefore, the $\mathrm{SNR_{in}}$ is defined as the signal power in each subband proportion to the noise power in the entire Nyquist range.

We use two methods to analyse the reconstruction algorithm performance. Since reconstructing the support S is essential for the MUSIC algorithm, one method is to evaluate the probability of finding the correct support. Another is the MSE. Here we evaluate the MSE between the reconstructed signal spectrum and the spectrum sampled at Nyquist rate.

Fig. 1b shows the benchmark of MUSIC algorithm at $\mathrm{SNR_{in}} = 100\,\mathrm{dB}$ and $p = 6$. The x-axis shows the number of simulations, and the y-axis shows the spectrum MSE. The simulation stops when the following condition is met for 5 times consecutively, i.e. the difference between the ith MSE and j^{th} MSE is smaller than 1×10^{-3}, where $j = i + 100$, $i \in \mathbb{Z}^+$, and $i \geq 5000$. In this paper, the number of simulations for each set-up is no less than 5000 times. Fig. 1b shows that after around 11000 simulations, the spectrum MSE is 0.0068.

4.2 Recovery Probability

Fig. 2 shows a comparison between probability of finding the correct spectrum support vs. the number of samplers. The x-axis is the number of samplers p, where the sampling rate is $f_s = p/LT$, and 50 samplers corresponds to the Nyquist rate.

It is not surprising to see that the more samplers, the higher probability of correct reconstruction can be achieved. Comparing the $30\,\mathrm{dB}$ cases, MUSIC is the best. It can achieve the theoretical lowest sampling rate when $p = 6$. We get the same perfect reconstruction from M-StOMP, and M-BPDN when $p = 11$, and $p = 12$ respectively. So, the advantage of MUSIC is obvious. Comparing with M-StOMP

and M-BPDN, it looks similar. By checking the lowest number p for which $P = 100\%$ at different $\mathrm{SNR_{in}}$, we find that M-StOMP works slightly better than M-BPDN. The simulation result is the same as the theoretical result in [5]. With decreased $\mathrm{SNR_{in}}$, if the signal is heavily distorted by noise ($\mathrm{SNR_{in}} < 0\,\mathrm{dB}$), MUSIC is not better than the other two algorithms. The reason is that for MUSIC, when the signal is drowned out by the noise, it is difficult to separate the signal subspace from the noise subspace by the eigenvalues in (9).

4.3 Mean Square Error

Having found the correct spectrum support, we evaluate the reconstructed spectrum quality. Fig. 3 shows three images representing the spectrum MSE. Along the x-axis is the number of samplers p, and along the y-axis is $\mathrm{SNR_{in}}$ from $-8\,\mathrm{dB}$ to $30\,\mathrm{dB}$. The step size of the y-axis is $1\,\mathrm{dB}$. Each pixel represents a MSE value. The three images use the same grey scale from 0 to 0.25. Here we define 0 as black (perfect reconstruction), and 0.25 as white (failed reconstruction).

Comparing Fig. 3a to 3c, it is quite clear to find a narrow line in (a) as the lowest sampling rate to separate successful and failed reconstruction from $30\,\mathrm{dB}$ to $5\,\mathrm{dB}$. However, in (b) and (c), the boundary of lowest sampling rate is blurred. In the region of $0\,\mathrm{dB} \leq \mathrm{SNR_{in}} \leq 5\,\mathrm{dB}$, MUSIC still works significantly better than M-StOMP, and M-BPDN, if the number N in (9) is given.

However, the performance of the MUSIC algorithm is strongly related to steps 3 and 5 in Algorithm 1. First, when the number of N is unknown, we cannot take the first $2N$ eigenvalues arbitrarily as signal subspace. The algorithm works only if signal eigenvalues are separable from noise eigenvalues, which requires an obvious gap between these two groups of eigenvalues. Second, the support set S is determined by the peak indices in step 5. Therefore, the method of designing the thresholding for $\hat{P}_{mu}$ is very important.

When $\mathrm{SNR_{in}} < 0\,\mathrm{dB}$, the MSE in both (b) and (c) are decreased with increased number of samplers except for MUSIC. In this region, MUSIC seems to fail. Even when sampling the signal at Nyquist rate, M-BPDN can reconstruct the signal successfully at $\mathrm{SNR_{in}} = -8\,\mathrm{dB}$ while M-StOMP and MUSIC cannot. In the case of MUSIC, the difficulty lies in signal and noise eigenvalue separation. For the M-StOMP algorithm, with increased noise level, the algorithm is easily attracted by local minima. Meanwhile, although M-BPDN works well when $\mathrm{SNR_{in}} \leq 0\,\mathrm{dB}$, the performance of the algorithm is determined by the level of the coefficient ϵ in (4). Usually the $\mathrm{SNR_{in}}$ is unknown in advance, which makes M-BPDN sensitive to inaccurate estimation of δ_ϵ^2 in (11).

5. CONCLUSION

In this paper, we analyzed three multiple measurement vector (MMV) reconstruction algorithms, namely as MUSIC, M-StOMP, and M-BPDN, for blind reconstruction of multiband signals from samples below the Nyquist rate. M-StOMP is a paralleled greedy pursuit algorithm, and M-BPDN is a paralleled basis pursuit de-noising algorithm. After evaluating numerous simulations, we see that MUSIC can achieve the theoretical lowest sampling rate when $\mathrm{SNR_{in}} \geq 30\,\mathrm{dB}$. We also identify that it is a bottleneck for MUSIC to separate the signal and noise eigenvalues when $\mathrm{SNR_{in}} \leq 0\,\mathrm{dB}$. For M-StOMP, and M-BPDN, we find M-StOMP to outperform M-BPDN in all tested cases. However, when $\mathrm{SNR_{in}} < 0\,\mathrm{dB}$,
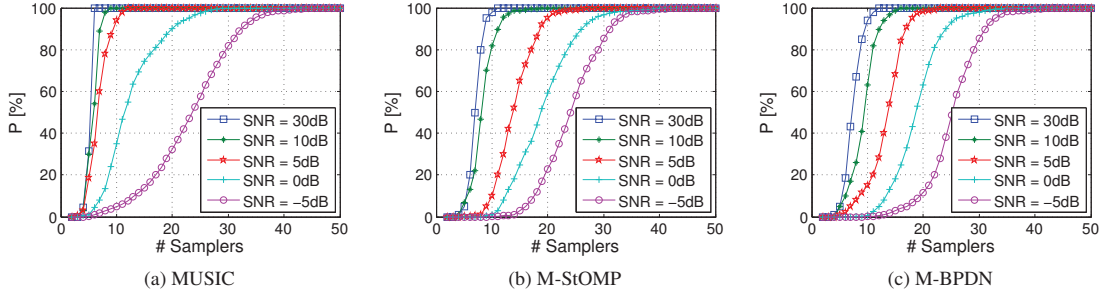
Figure 2: Probability of finding correct spectrum support vs. no. of samplers. (a) MUSIC Recovery Probability. (b) M-StOMP Recovery Probability. (c) M-BPDN Recovery Probability.
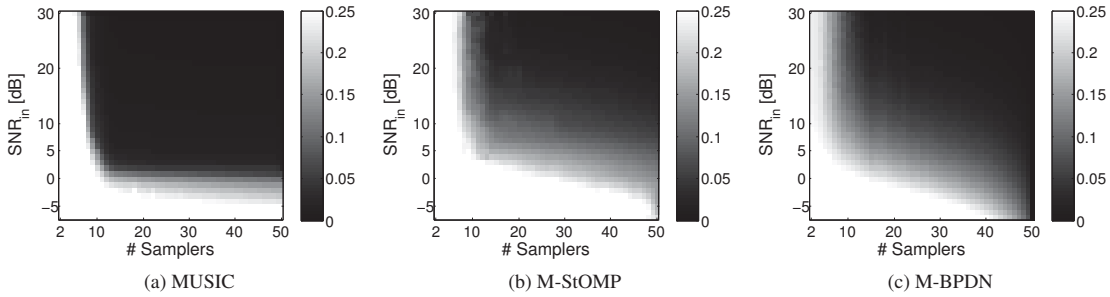

Figure 3: SNR_{in} vs. no. of samplers on grey map, the pixel color is proportional to the MSE of reconstructed signal. (a) MUSIC Recovery MSE Performance. (b) M-StOMP Recovery MSE Performance. (c) M-BPDN Recovery MSE Performance.

the M-BPDN is the only algorithm which can reconstruct a signal successfully at the Nyquist rate.

Future work can be focused on the sampling matrix **A** design or reconstruction algorithm improvement. It's not trivial to design a universal sampling matrix (5). Meanwhile, eigenvalue separation is crucial for MUSIC when SNR_{in} is low, and N is unknown.

REFERENCES

[1] S. Mallat, *A wavelet tour of signal processing – the sparse way*. Academic Press, Third Edition, Burlington, MA, USA, 2009.

[2] E. Candès and M. Wakin, "An introduction to compressive sampling," *IEEE Signal Process. Mag.*, vol. 25, no. 2, pp. 21–30, 2008.

[3] P. Feng and Y. Bresler, "Spectrum-blind minimum-rate sampling and reconstruction of multiband signals," in *IEEE International Conference on Acoustics Speech and Signal Processing*, vol. 3, pp. 1688 –1691, 1996.

[4] M. Mishali and Y. C. Eldar, "Blind multiband signal reconstruction: compressed sensing for analog signals," *IEEE Trans. Signal Process.*, vol. 57, no. 3, pp. 993–1009, 2009.

[5] J. Chen and X. Huo, "Theoretical results about finding the sparsest representations of multiple measurement vectors (MMV) in an overcomplete dictionary using l1 minimization and greedy algorithms," *IEEE Trans. Signal Process.*, vol. 54, no. 12, pp. 4634–4643, 2006.

[6] R. Schmidt, "Multiple emitter location and signal parameter estimation," *IEEE Trans. Antennas Propag.*, vol. 34, no. 3, pp. 276–280, 1986.

[7] E. van den Berg and M. P. Friedlander, "SPGL1: A solver for large-scale sparse reconstruction," June 2007. http://www.cs.ubc.ca/labs/scl/spgl1.

[8] T. Blumensath and M. Davies, "Stagewise weak gradient pursuits," *IEEE Trans. Signal Process.*, vol. 57, no. 11, pp. 4333–4346, 2009.

[9] R. Venkataramani and Y. Bresler, "Perfect reconstruction formulas and bounds on aliasing error in sub-nyquist nonuniform sampling of multiband signals," *IEEE Trans. Inf. Theory*, vol. 46, no. 6, pp. 2173–2183, 2000.

[10] J. Tropp, J. Laska, M. Duarte, J. Romberg, and R. Baraniuk, "Beyond Nyquist: efficient sampling of sparse bandlimited signals," *IEEE Trans. Inf. Theory*, vol. 56, no. 1, pp. 520–544, 2009.

[11] S. Chen, D. Donoho, and M. Saunders, "Atomic decomposition by basis pursuit," *SIAM J. Sci. Comput.*, vol. 20, no. 1, pp. 33–61, 1998.

[12] J. Tropp, "Greed is good: algorithmic results for sparse approximation," *IEEE Trans. Inf. Theory*, vol. 50, no. 10, pp. 2231–2242, 2004.